International Journal of Sustainable Energy and Environmental Research
2017 Vol. 6, No. 1, pp. 9-26
ISSN(e): 2306-6253
ISSN(p): 2312-5764
DOI: 10.18488/journal.13.2017.61.9.26

SIMULATION OF SOLAR PHOTOVOLTAIC, BIOMASS GAS TURBINE AND DISTRICT HEATING HYBRID SYSTEM

S. Sami[1+]
E. Marin[2]

[1,2]*Research Center for Renewable Energy Catholic University of Cuenca, Cuenca, Ecuador*


(+ Corresponding author)

Article History
Received: 14 December 2016
Revised: 16 January 2017
Accepted: 22 February 2017
Published: 9 March 2017

Keywords
Integrated-gas turbine biomass system
CHP
Modeling
Simulation
Experimental validation.

ABSTRACT

This paper presents a simulation model for Biomass-Photovoltaic Hybrid system. The energy conversion equations describing the total power generated by system have been presented. A numerical model based upon the aforementioned conservation equations was developed, coded and results were presented and analyzed. The model is intended to be used as an optimization, design and analysis tool for typical gas turbine Biomass-CHP hybrid systems. The results predicted by the proposed model compared fairly with data under various biomass loading conditions.

Contribution/ Originality: This study contributes to the existing literature of photovoltaic, biomass and district heating hybrid systems. This study uses a new approach in modeling the hybrid system by establishing the conservation and conversion equations, integrating, coding and solving them to obtain the dynamic behavior of the hybrid system.

1. INTRODUCTION

Gas turbines have long been used to produce power and are the main source of power for many applications such as jet aircraft and industrial power plants. The basic components of a gas turbine are a compressor, combustor or heat exchanger, and a turbine. The compressor is typically an axial flow or centrifugal design. The concept is similar to that of a combustion engine where the chemical energy of a fuel is converted into mechanical energy. A working fluid (usually air) is compressed, fuel is added in the combustion chamber and the mixture is ignited to initiate combustion as shown in Figure. 1. The combustion process releases energy and flue gases that expand in the gas turbine which is the mechanical work out of the cycle. A portion of this mechanical energy is also used to drive the compressor. The difference between the power to drive the compressor and the total power out of the turbine is the net power produced by the cycle. This paper is concerned with a hybrid system with a Solar

+ Corresponding author

Photovoltaic gas turbine where is the solar Photovoltaic powers the compressor. In turn this will enhance the hybrid system's output power and total efficiency. Renewable and nonconventional methods of power generation such as wind, solar, hydraulic, biomass, geothermal, thermal storage and waste heat recovery power generations offer power supply solutions for remote areas that are not accessible by grid power supply (Department of Energy, 2007; Kavitha and Kamdi, 2013; Mustafa, 2013; Binayak *et al*., 2014).

Hybridization between solar source and gas turbines have been presented (Sinai *et al*., 2005; Solgate, 2005; Heller *et al*., 2006; Korzynietz *et al*., 2012; Camerettia *et al*., 2015) using solar tower and field installed at Platform Solar de Almería (Spain). Where, solar hybrid power system was used with direct solar heating of pressurized air.

Furthermore, a computer simulation model of the behavior of photovoltaic PV and gas turbine hybrid system with compressed air storage was presented by Jaber (2004) to evaluate and predict performance of the total energy conversion efficiency under different operating conditions. He reported that his integrated PV gas turbine hybrid system produced approximately 140% more power compared to conventional gas turbine plants power.

The concept of integrated PV gas turbine hybrid system where the solar PV panels drive the compressor is hereby presented as an innovative technique to enhance the hybrid system energy conversion efficiency. This paper is concerned with the main heat and mass transfer mechanisms in the gas turbine combustion chamber such as convection, conduction and moist content evaporation as well as the analysis of solar photovoltaic integrated and district heating hybrid system. A numerical simulation using one dimensional model is presented herein to describe the hybrid system in question and its performance under different conditions.

2. MATHEMATICAL MODELING

In the following sections, the energy conversion equations for each source of renewable energy to an electrical energy are presented;

2.1. Biogas Gas Turbine Model

In the hybrid system, ambient air is compressed and supplied to the combustion chamber

The compressor model is based on the perfect gas equations and polytropic transformations (Chinda and Brault, 2012)

The exhaust temperature:

$$T_e = T_i \left(\frac{P_e}{P_i}\right)^{\frac{(\gamma a-1)}{\gamma a \eta_{\infty c}}} \quad (1)$$

Where, i is inlet, e is exit, P is pressure, T is temperature, □*a* = *Cpa/Cva* or ratio of specific heats of air and □□*C* is polytropic efficiency of the compressor.

Meanwhile the change in isentropic enthalpy during the compression is:

$$\Delta h_c = C_{pa} T_i \left(\frac{P_e}{P_i}\right)^{\frac{R_a}{Cpa}} - 1 \quad (2)$$

Efficiency of the compressor can be obtained as follows;

$$\eta_C = \frac{1-\left(\frac{P_e}{P_i}\right)^{\left(\frac{\gamma a-1}{\gamma a}\right)}}{1-\left(\frac{P_e}{P_i}\right)^{\left(\frac{\gamma a-1}{\gamma a \eta_{\infty c}}\right)}} \quad (3)$$

The mechanical power consumed by the compressor is obtained after the following equation;

$$Wpc = \frac{q_{air}\,\Delta h_c}{\eta_c\,\eta_{trans}} \quad (4)$$

Where *qair* is the air flow rate in kg/s and □ is the transmission efficiency from turbine to compressor.

The turbine is modeled similar to the aforementioned compressor model with uniform polytropic expansion.

The turbine exhaust temperature is obtained as follows;

$$T_e = T_i \left(\frac{P_e}{P_i}\right)^{\frac{(\gamma g-1)}{\gamma g \eta_{\infty TG}}} \quad (5)$$

Where, i is inlet, e is exit, P is pressure, T is temperature and c_{pa} / c_{va} is ratio of specific heats of combustion gases and TG is polytropic efficiency of the turbine.

Once can calculate the change in isentropic enthalpy across the turbine as;

$$\Delta h_{TG} = C_{pg} T_i \left(\frac{P_e}{P_i}\right)^{\frac{R_g}{C_{pg}}} - 1 \quad (6)$$

The gas turbine efficiency is:

$$\eta_{TG} = \frac{1-\left(\frac{P_e}{P_i}\right)^{\left(\frac{\gamma_a-1}{\gamma a \eta_{\infty TG}}\right)}}{1-\left(\frac{P_e}{P_i}\right)^{\left(\frac{\gamma g-1}{\gamma g}\right)}} \quad (10)$$

The total mechanical power generated by the gas turbine can be calculated as:

$$W_{TG} = \eta_{TG} q_{TG} \Delta h_{TG} \quad (11)$$

Finally, net mechanical power delivered to produce electricity:

$$W_{GTN} = W_{TG} - Wpc \quad (12)$$

2.2. District Heating Model

Hybrid system district heating heat exchanger is modeled as a parallel flow;

$$\Delta T_1 = T_{h,1} - T_{c,1} \quad (13)$$

$$\Delta T_2 = T_{h,2} - T_{c,2} \quad (14)$$

Where, $T1$ and $T2$ are the hot and cold flows temperature differences at the entrance and exit of the heat exchanger, respectively.

$$q = UA\Delta T_{lm} \quad (15)$$

Where Tlm is the log mean temperature difference (LMTD) and defined as;

$$\Delta T_{lm} = \frac{\Delta T_2 - \Delta T_1}{\ln(\frac{\Delta T_2}{\Delta T_1})} \quad (16)$$

Where U and A are the overall heat transfer coefficient, and total heat transfer area of the heat exchanger, respectively.

2.3. Combustion Chamber Model

In the following the heat and mass transfer model is presented for the combustion chamber model. The flue gases are released after the biogas combustion. The radiation is the major heat transfer by-product because of the high temperature of the gas. However, other heat transfer mechanisms are present in the furnace heat transfer such as convective, evaporation and combustion and must be taken in consideration in order to solve the energy conversion equations of biomass incinerators (Saravanautto *et al.*, 2001; Fargali *et al.*, 2008; Chinda and Brault, 2012; Sami and Marin, 2017)

$$Q_{add_{gas}} = Q_{comb} + Q_{rad} - Q_{conv} - Q_{evap} \quad (17)$$

Where;

$$Q_{add_{gas}} = m_{gas} C_{pgas} (T_{out} - T_{air}) \quad (18)$$

$$Q_{add} = 4.18 CV_{bio} m_{bio} \eta_{heater} \quad (19)$$

$$Q_{conv} = h_w A_{wall} (T_{gas} - T_{well}) \quad (20)$$

$$Q_{rad} = E_g A(T4_a - T4_{bed}) \quad (21)$$

$$Q_{evap} = \eta_{water} H_{evap} \quad (22)$$

As shown in Figure .1, the hot flue gases emitted from the gas turbine combustion chamber are forwarded and expanded in the gas turbine and in turn the flue gases exhausted from the gas turbine are used to produce hot water for district heating applications.

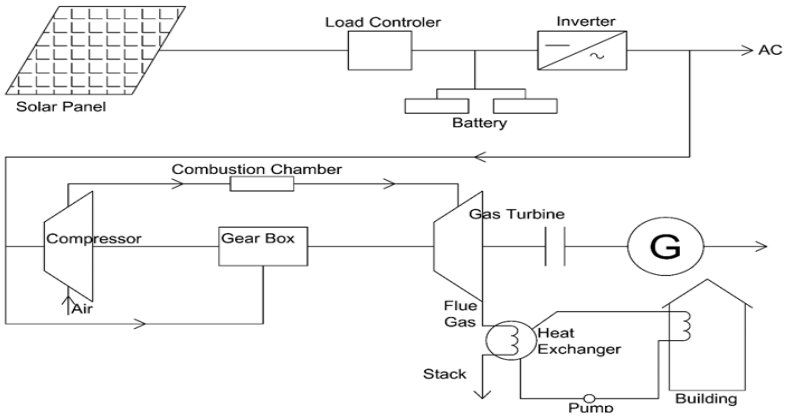

Figure-1. Biogas integrated Gas Turbine PV hybrid system.

The total gas turbine out power is obtained as follows;

$$W_{GT} = \eta_{GT}\, m_{fg}(h_1 - h_2) \quad (23)$$

The total district heating load can be calculated as follows;

$$Q_{ed} = \eta_{WH}\, m_w(h_d - h_L) \quad (24)$$

Where h_1, h_2 represent the flue gas inlet and outlet enthalpies at the gas turbine respectively. And h_d, h_L are the hot water enthalpies at inlet and outlet of the heat exchanger tank.

The heat balance at the building water heater tank heat exchanger is as follows;

$$m_w C_w(T_d - T_L) = \eta_{HX}\, m_{fg}(h_3 - h_4) \quad (25)$$

Where h_3, h_4 are the flue gas inlet and outlet enthalpies at the heat exchanger tank, respectively,

The net gas turbine efficiency is obtained as follows;

$$\eta_{GTS} = \frac{W_{GTN}}{Q_{comb}} \quad (26)$$

Equation (26) defines the net biomass gas turbine efficiency that includes all losses and power consumed by accessories such as the compressor.

On the other hand, the energy balance at the biomass flue gas district heater (Korzynietz *et al.*, 2012; Mustafa, 2013) can be used to estimate the hot water temperature time-variation in the heater tank to be used for district heating as follows;

$$dT/dt_w = \frac{m_{gas} C_{pgas}(T_{in_w} - T_{out_w})}{V_{tank}\delta_w C_{p_w}} - \frac{m_w C_{p_w}(T_d - T_L)}{V_{tank}\delta_w C_{p_w}} \quad (27)$$

Where,

Q_{comb}: Combustion heat added to gas turbine combustion chamber

Q_{rad}: Radiative heat

Q_{conv}: Convective heat

Q_{evap}: Evaporative heat

T: is the temperature water in heat exchanger tank

δ_w: Density of water

V_{tank}: Volume of heater

m_{fg}: Mass flow rate of flue gas

m_{gas}: Biomass waste mass material

m_w: Mass flow rate water

Q_{ed}: Building heat load

η_{GTS}: Net Gas Turbine thermal efficiency

Finally the hybrid system Biomass-Gas turbine and district heating energy conversion efficiency can be obtained as follows;

$$\eta_{biogas} = \frac{W_{GTN+Qed}}{Q_{comb}} \quad (28)$$

Where Q_{comb} is defined as follows;

$$Q_{comb} = 4.18 CV_{bio} m_{bio} \eta_{bio} \quad (29)$$

Where;

CV_{bio}: Calorific heat value of bio-gas

η_{bio}: Biogas combustion chamber efficiency

2.4. Solar Photovoltaic Model

The solar photovoltaic panel is made of modules and each module is consisted of arrays and cells. The dynamic current output can be obtained as follows (Saravanautto *et al.*, 2001; Fargali *et al.*, 2008; Sami and Marin, 2017)

$$I_p = I_L - I_o \left[\exp\left(\frac{q\,(V+I_p\,R_s)}{A\,k\,T_C}\right) - \left(\frac{(V+I_p\,R_s)}{R_{sh}}\right)\right] \quad (30)$$

And

$$Io = BT^3{}_C \left[\exp\left(-\frac{E_{go}}{K\,T_C}\right)\right] \quad (31)$$

$$I_L = P_1 G[1 - P_2(G - G_r) + P_3(T_C - T_r)] \quad (32)$$

Where;

The PV cell temperature T_c is influenced by several factors such as solar radiation, ambient conditions, and wind speed. This parameter impacts the PV output current, and its time-variation can be determined from the following (Yang *et al.*, 2007; Korzynietz *et al.*, 2012)

$$\left(m\, C_{p_{module}}\right)\frac{dT_C}{dt} = Q_{in} - Q_{conv} - Q_{elect} \quad (33)$$

Where;

$$Q_{in} = \alpha_{abs} G S_p \quad (34)$$

$$Q_{conv} = S_p H(T_C - T_a) \quad (35)$$

$$Q_{elect} = \eta G S_C \quad (36)$$

$$H = 1.2475\,(\Delta T \cos\beta)^{\frac{1}{3}} + 2.685u \quad (37)$$

$$\eta = \eta_o[1 - \gamma(T_C - T_r)] \quad (38)$$

Where u and G are the wind speed and solar radiation and S_p represents the solar panel area.

3. NUMERICAL PROCEDURE

The energy conversion and heat transfer mechanisms taking place during the various processes shown in Figure.1, are described in equations (1) through (22). These equations have been solved as per the logical flow diagram presented in Figure. 2, where the input parameters of Biomass gas turbine, PV and the district heating as well as the various independent parameters are defined. Dependent parameters were calculated and integrated in

the system with the finite-difference formulations. Iterations were performed until a solution is reached with acceptable iteration error.

The numerical procedure starts with using the biogas flow rate and air flow to calculate the mass flow rate of flue gas, and hot water flow rate circulating in the various loops under specified conditions. The thermodynamic and thermo physical properties of flue gas and hot water are determined based upon the initial conditions of the air and biogas flow, and excess air ratio. This is followed by using the finite-difference formulations to predict the time variation of the hot water temperature as per equation (27) and PV cell temperature as per equation (33) as well as other hybrid system power outputs and efficiencies. Finally, hybrid system efficiency is calculated at each input condition.

4. RESULTS AND DISCUSSION

In order to solve the aforementioned equations (1) through (38) and taking into account that total power may not be simultaneous, and for validation purposes, this simulation model and the above mentioned equations were coded with finite-difference formulations. In addition, for the purpose of validation and tuning up the predicted output simulated results, the data was used to validate the simulation program under various conditions. In the following sections, we present analysis and discussions of the numerical results predicted as well as validations of the proposed simulation model.

4.1. Biomass Simulation

Equations (1) through (28) present the heat and mass calculation balance at the gas turbine, combustion chamber where the biogas is fed to the combustion chamber and the combustion process releases heat which is converted to the gas and ash through chemical reactions. The air flows to the compressor vary from 136.95 to 400 kg/s in this study with compressor entering temperature ranging from 288 to 481 K. It was assumed that the fuel air ratio was 0.10 and the maximum excess air ratio was 120% during the combustion process (Saravanautto *et al.*, 2001). This is necessary to maintain the combustion chamber temperature exit within the range of 1433 °K to ensure complete combustion.

The predicted results of the biomass simulation at different conditions are presented in Figures 3 through 11. In particular, Figures. 3 and 4 depict the biomass output power at various conditions of air compressor flow rates, gas turbine efficiency and hybrid system efficiency as well as the use of PV solar panels as a driver to the air compressor of the gas turbine system.

It is apparent from these figures that increasing air flow and consequently the flue gas flow rate enhances the output power produced by the gas turbine system and hybrid system. Furthermore, the higher the air flow rate the higher the efficiency of the gas turbine system with the compressor driven by PV solar panels. However, when taking into account the solar radiation converted by the solar panels the hybrid system efficiency diminishes with increasing the air compressor flow rate.

Figures 5 and 6 have been constructed to illustrate the impact of increasing the air flow temperature entering the compressor on the gas turbine performance while the compressor is driven by the PV solar at solar radiation of 1000 w/m^2 and 0% excess air. The results displayed in these figures show that the higher the temperature of air flow rate entering the compressor the higher the power produced and the higher power consumed by compressor. This consequently increases the solar PV power required to drive the compressor. In addition, Figure.6 also shows that the higher the air compressor flow rate the higher the heat of combustion added in the gas turbine combustion chamber to ensure full combustion.

Figure 7 and 8 present the effect of solar PV panels on the efficiency of the hybrid system, at 1000 w/m^2 and 0% excess air ratio, where, the hybrid system efficiency was calculated using equation (28) based upon standard air conditions and plotted with and without taking into account the PV solar panels that drive the compressor. It is

quite evident from these figures that taking account of the solar powered PV panels as an input energy reduces the hybrid system efficiency at higher compressor air flow. This is due to the fact that higher air compressor air flow requires significantly more power to drive the compressor as illustrated in equation (12). Furthermore, Figure.8 also shows a comparison between the efficiencies of hybrid system calculated by equation (28) based upon the gas turbine net output [equation (12)] and that of the gas turbine output [equation (23)].

To maintain the gas turbine combustion chamber within full burn condition, the flue gas temperature must be within 850-950°C. The exit temperature of the flue gas of the gas turbine combustion chamber burner requires more combustion and excess air ratios higher than 100% for theoretical combustion (i.e. 0% excess air). This implies supplying excess air. Theoretically, the higher the excess air ratio the lower the temperature of the combustion flue gas (Yang *et al.*, 2007). Therefore, it is necessary to optimize the excess air ratio. Towards that end, Figures 9 through 11 have been constructed to study the impact of excess air ratios on the efficiencies of gas turbine, and the hybrid system that includes gas turbine, PV solar panels and district heating. Excess air ratios considered in this study are 10% through 40% as shown in Figures 9 through 11. It can be observed from the simulation results displayed in these figures that the higher the excess air ratio the lower the efficiency. This can be attributed to the increase of the compressor power and reduction of the combustion gases temperature and consequently to less power generated at the gas turbine generator. On the other hand, in general, the simulated results under these conditions also show that the higher the compressor air temperature the higher the efficiency. In our opinion, this is attributed to higher compressor entering temperature leads to less heat of combustion in the combustion chamber and increase in the efficiency. However, Figure 11 shows also that the higher the compressor entering temperature the lower the hybrid system efficiency due to the higher solar PV input to the compressor. Also the results displayed in this figure show that the higher the excess air ratio the lower the efficiency. Similar behavior was observed with other air flow rates. It is also believed that increasing the air excess air increases the heat input at the combustion chamber and increases the heat losses and consequently the biomass energy conversion efficiency. Therefore, it appears from the aforementioned figures that the biomass power output is significantly influenced by the flue gas temperatures, air flow rates, and obviously the excess air ratios. Furthermore, the results also show that the maximum biomass output is achieved at higher air flow entering temperatures due to less power consumed by the compressor and consequently less solar PV panels required.

4.2. PV Simulation

Photovoltaic (PV) panels generate electricity directly from solar radiation/sunlight using an electronic process that converts solar radiation into electricity using certain types of material, called semiconductors. Electrons in semiconductors are freed by solar energy and travel through an electrical circuit, powering electrical devices. The basic concept of energy conversion from the solar insolation into electrical energy is shown in Figure.1. In this research work the PV solar panels as are an integral part of the hybrid system and employed to drive the compressor, therefore, enhancing the gas turbine and hybrid system efficiency. The PV solar panels characteristics and output hereby are analyzed in the following sections. Figures 12 through 15 illustrate the energy conversion from the solar insolation into electrical energy in terms of volts, amperes and power as a function of solar irradiance. It is quite clear, in particular, from figures 12 through 15 that the predicted PV characteristics are consistent with what has been reported in the literature (Fargali *et al.*, 2008; Mustafa, 2013; Sami and Icaza, 2015). Furthermore, in particular figure 14 shows that higher solar irradiance will result in higher energy conversion efficiency and output PV power. Therefore, the solar panels will be more efficient to operate at sites with higher solar irradiance.

Furthermore, in order to study the impact of the initial PV cell temperature on the energy conversion process using equation (33), Figures 16 and 17 have been constructed. It is worth noting that the numerical simulation presented hereby include the variation of PV cell temperatures from 10°C through 38°C. Furthermore, Figure 16

presents the PV energy conversion efficiency for different initial cell temperatures. The data presented in this figure also illustrate that the higher the initial cell temperature the higher the PV the PV energy conversion efficiency and power produced which is consistent with Fargali *et al.* (2008) and others.

The dynamic behavior of the PV cell can be predicted by equation (33). The time-variation of the PV cell temperature is shown in Figure 17 for different solar radiations during the day. It is quite clear from this figure that the maximum allowable cell temperature can be achieved depending upon the solar radiation. The higher the solar radiations the faster the increase in the PV cells temperature and these result in higher cell temperature. Therefore, utmost attention should be given to the time-variation of the PV cell temperature to avoid disintegration of the PV cell material.

4.3. Hybrid System Simulation

Furthermore, in order to demonstrate the impact of the most critical parameters affecting the hybrid system performance efficiency; the air flow rates and the solar radiations, Figures. 18 and 19 were constructed. Where, the hybrid system output power and its efficiency were plotted against compressor air flow at different solar radiations. In particular the hybrid system efficiency presented in Figure 19 takes into account the total output power and district heating load as per equation (28).

The number of PV solar panels was calculated to drive the compressor of the gas turbine at different conditions of air compressor flow rates at different solar radiations are displayed in Figure 20. The PV module characteristics and specifications employed were based upon data of Fargali *et al.* (2008) with total surface area of the PV module 0.99288 m^2. It is quite evident from the data presented in this figure that at a particular compressor air flow rate the higher the solar radiation the less number of solar panels needed to drive the compressor at that particular flow rate. On the other hand, the results displayed in this figure also demonstrate that the higher the compressor air flow rate the higher number of solar panel needed to drive the compressor. This is significant since the air flow rate impacts the output power at the gas turbine end and consequently the efficiency of the hybrid system.

4.4. District Heating Simulation

The biogas integrated gas turbine PV hybrid system presented in Figure.1 illustrates the district heating process where the flue gas exhausted from the gas turbine is used to supply heat load to a typical building. As can be seen from this figure the district heating load is impacted by the flue gas mass flow ate and its temperature, hot water temperature as well as the ambient temperature. To that end, Figure 21 has been constructed to illustrate the time-variation of the hot water feed temperature calculated by equation (27) during the district heating load at 136.95 kg/s air flow rate, solar radiation of 1000 w/m^2 and 0% excess air. It is quite evident from data displayed that the heat buildup accumulated in the hot water tank heat exchanger increases the hot water temperature. The desired temperature of hot water was reached after 1000 sec. This is important in designing the heat exchanger tank conditions to achieve the heat balance at the heat exchanger tank. Furthermore, similar behavior has been observed for other compressor air flow rates and solar radiations. However, it was also observed that the time to reach hot water desired temperature depends upon the compressor air flow, air intake temperatures and excess air ratios.

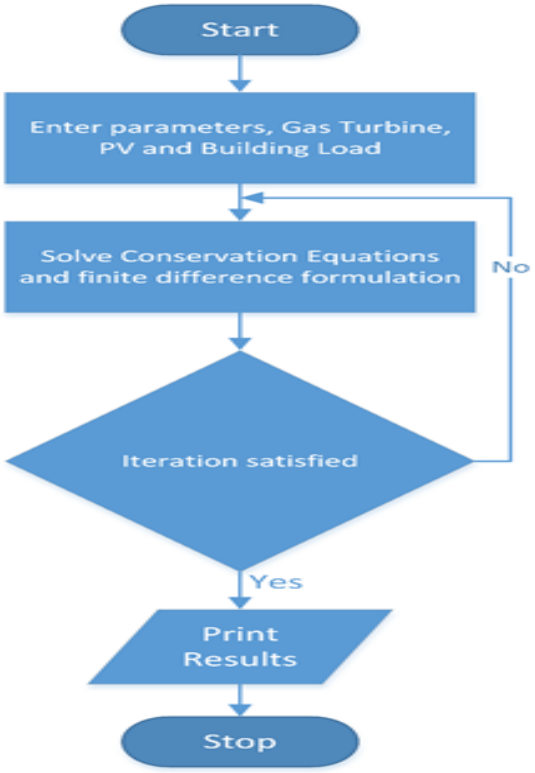

Figure-2. Logical flow diagram for numerical scheme.

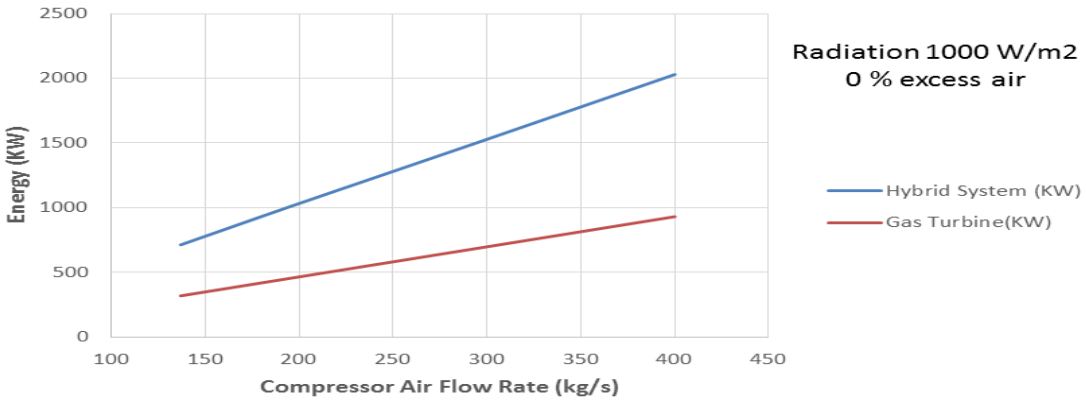

Figure-3. Biogas output power at different compressor air flow rates

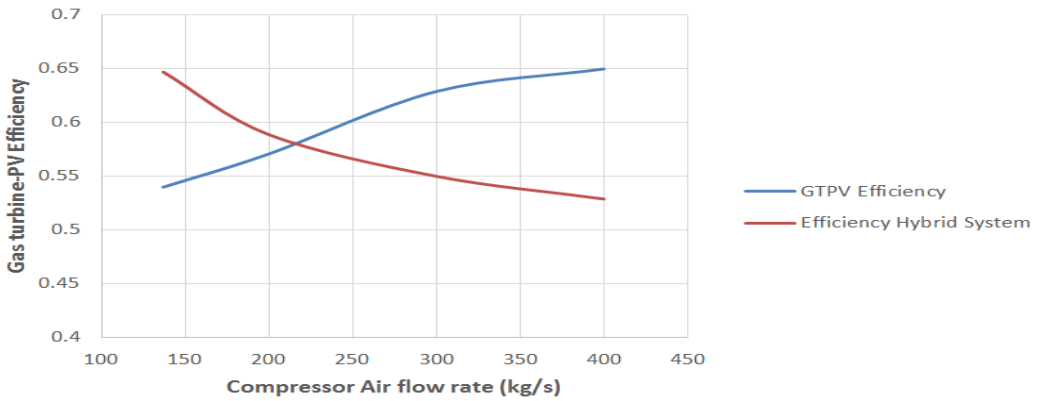

Figure-4. Biogas gas turbine efficiency different compressor air flow rates.

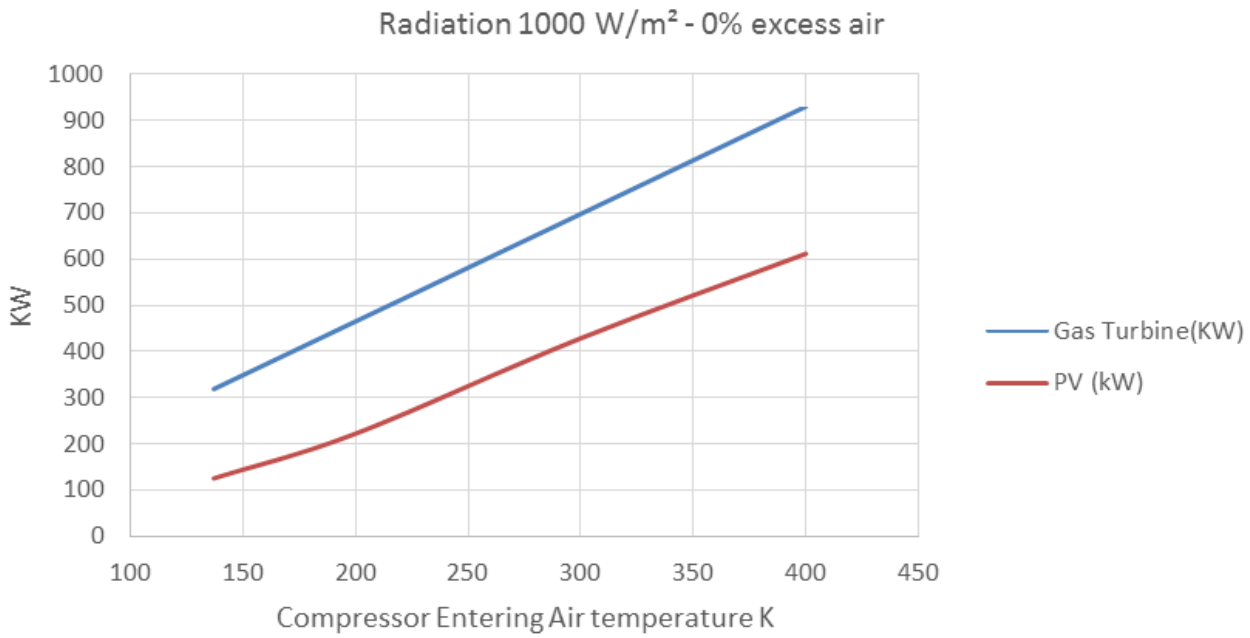

Figure-5. Biogas turbine output power at different compressor air entering temperature

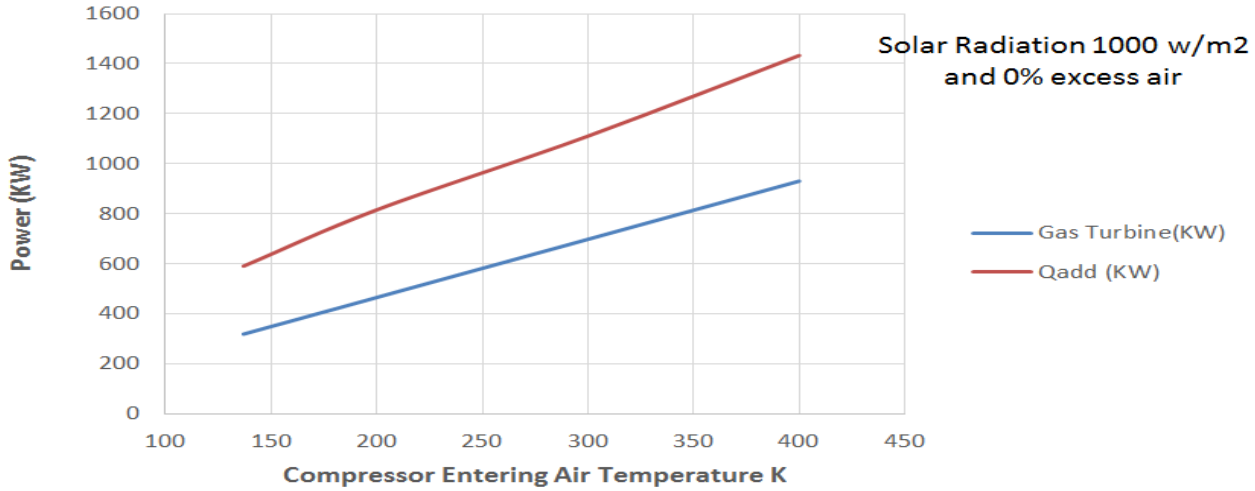

Figure-6. Biogas turbine output power at different compressor air entering temperature

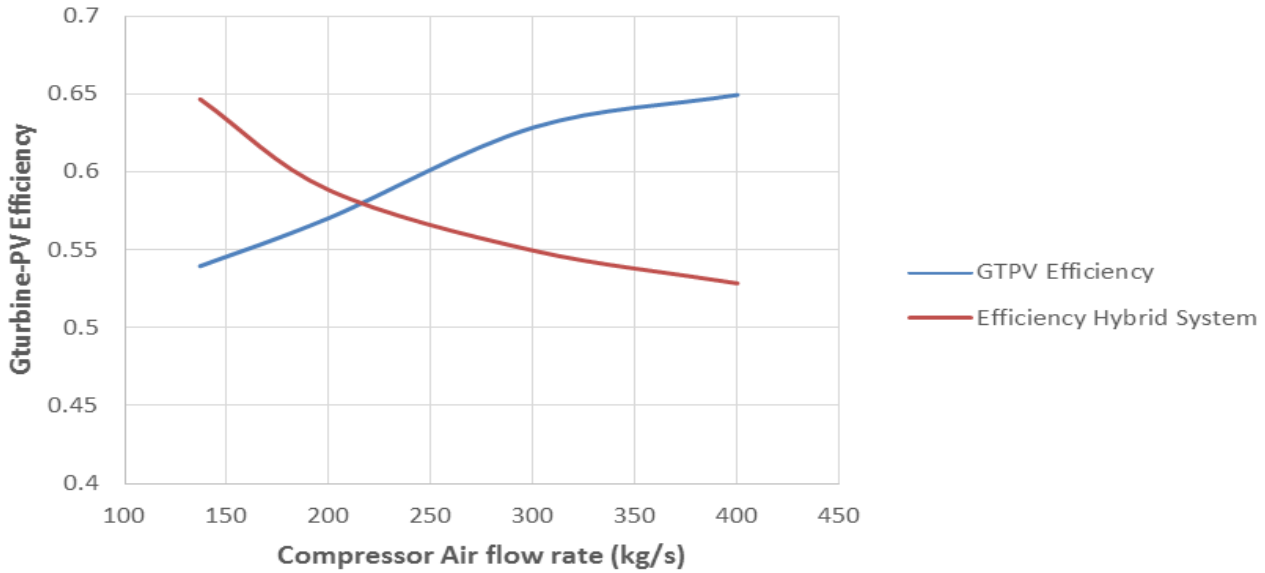

Figure-7. Efficiency of hybrid systems with and without solar energy for different compressor air flows.

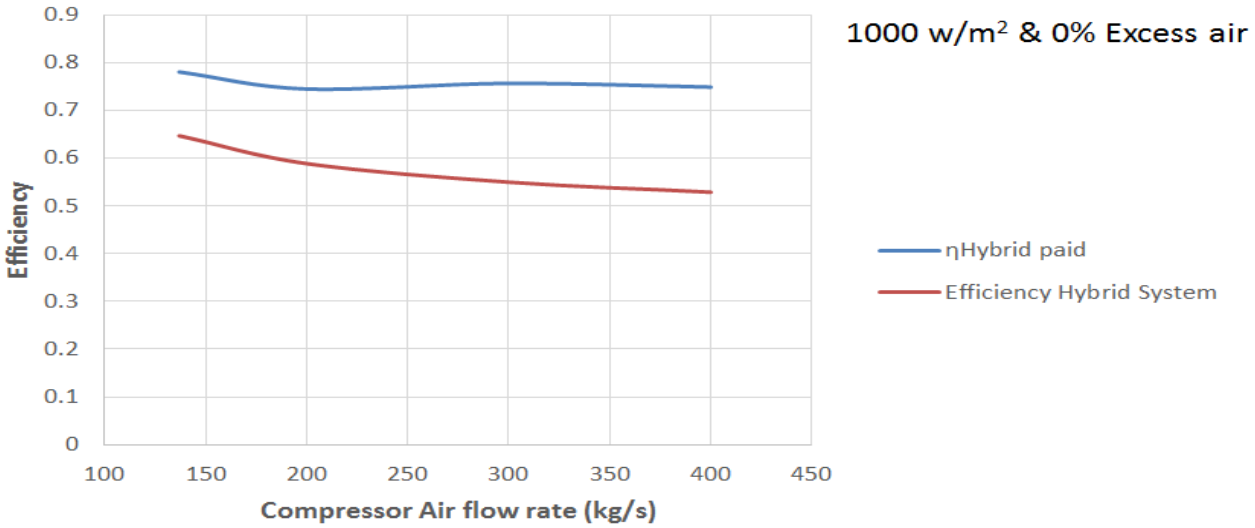

Figure-8. Efficiency of hybrid system with and without factoring solar energy cost

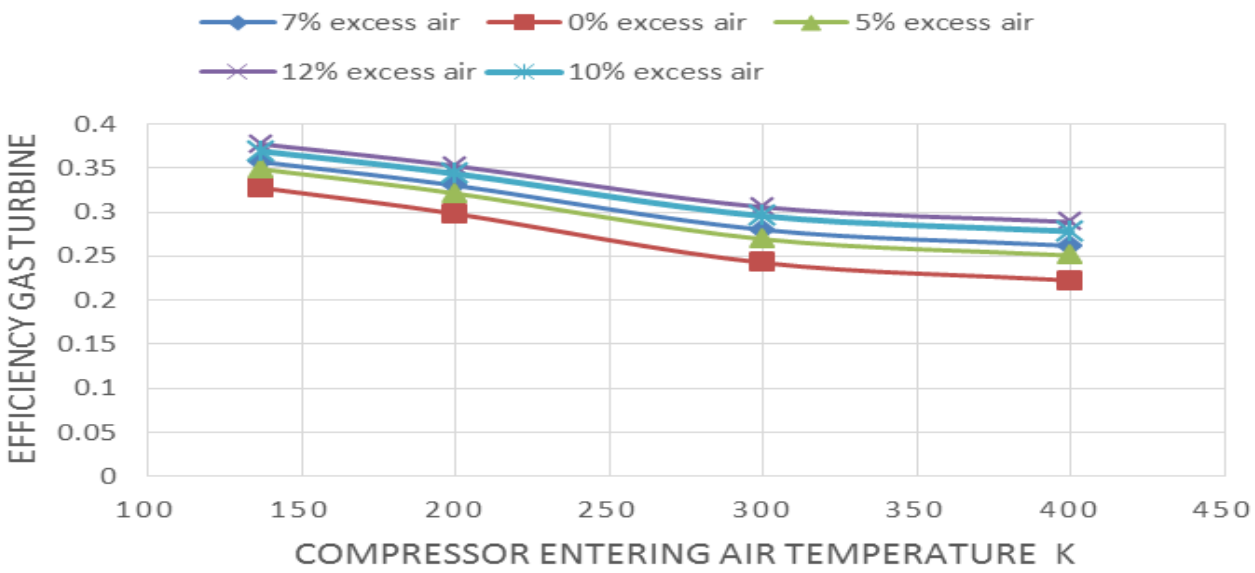

Figure-9. Biogas net power turbine efficiency at different compressor air entering temperature

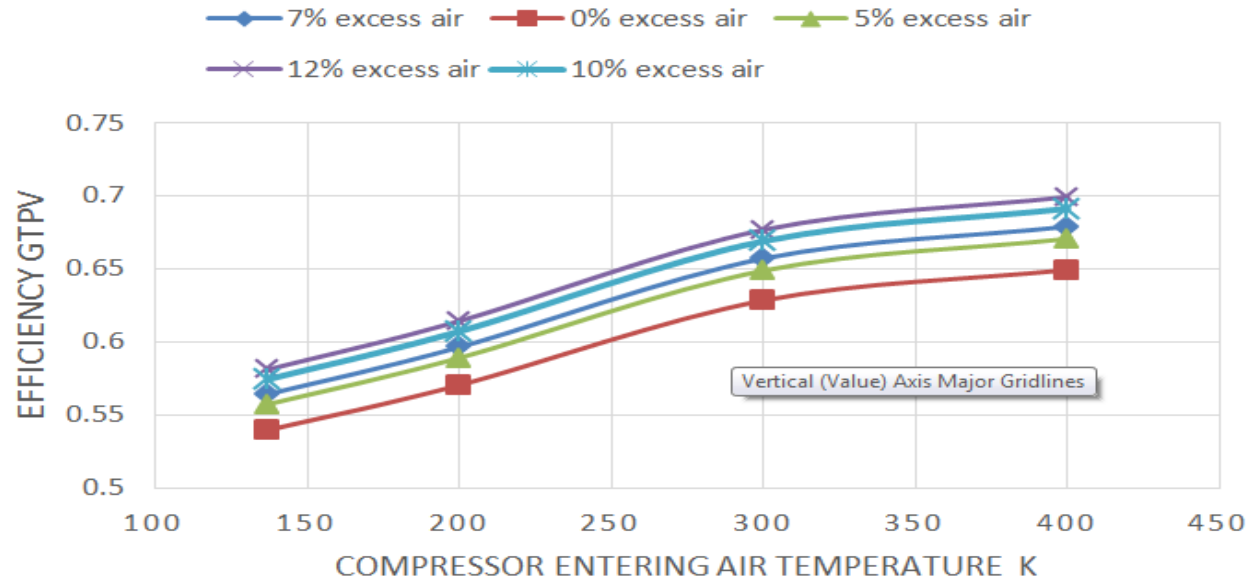

Figure-10. Efficiency of Biogas turbine with PV at different compressor air entering temperature

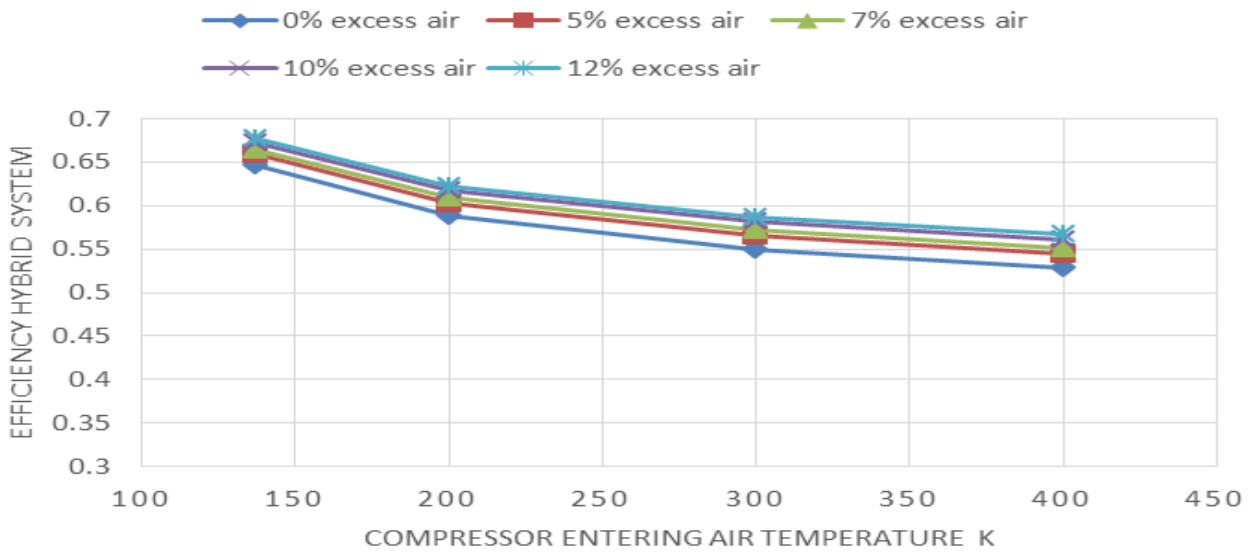

Figure-11. Efficiency of hybrid system; Biogas Turbine, PV, District heating at different compressor air entering temperature

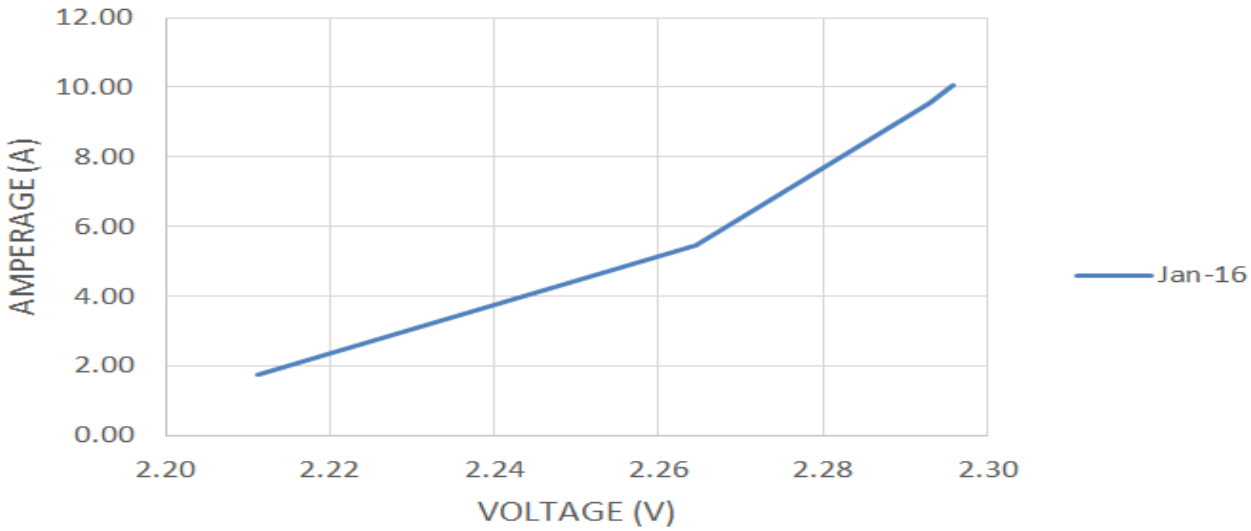

Figure-12. PV Characteristics: Amperage-Voltage

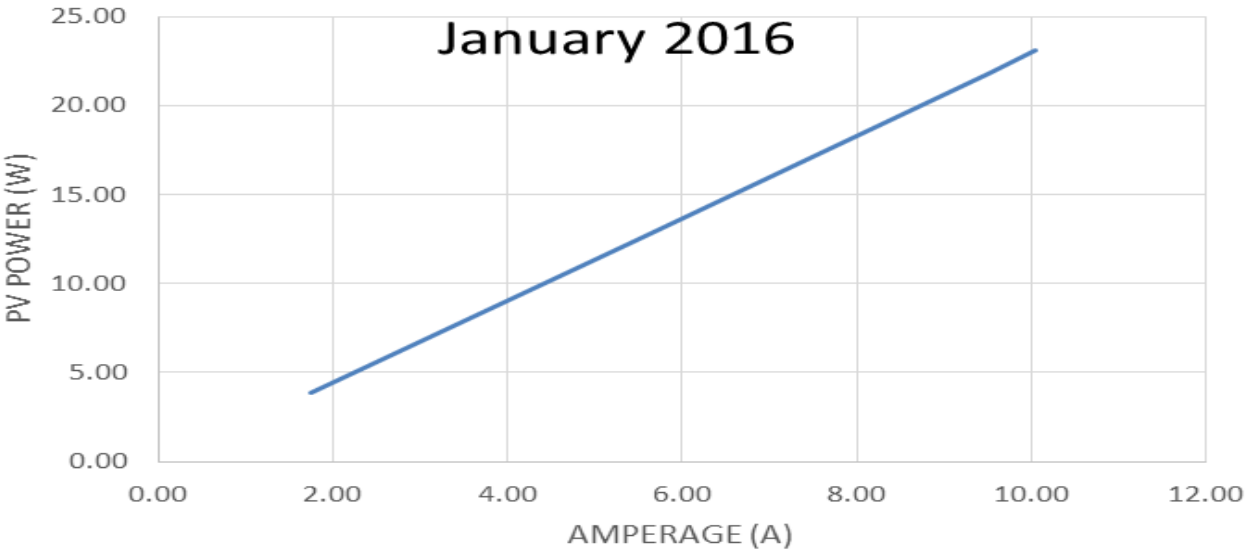

Figure-13. PV Characteristics: Amperage-Power

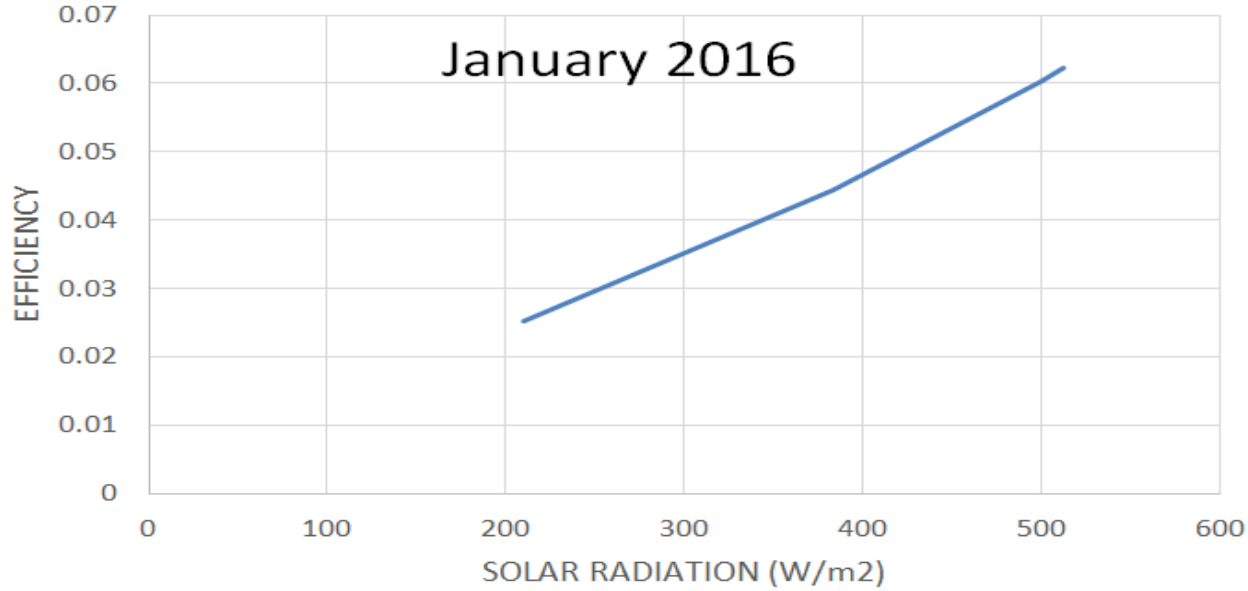

Figure-14. PV Characteristics: Efficiency -Radiation

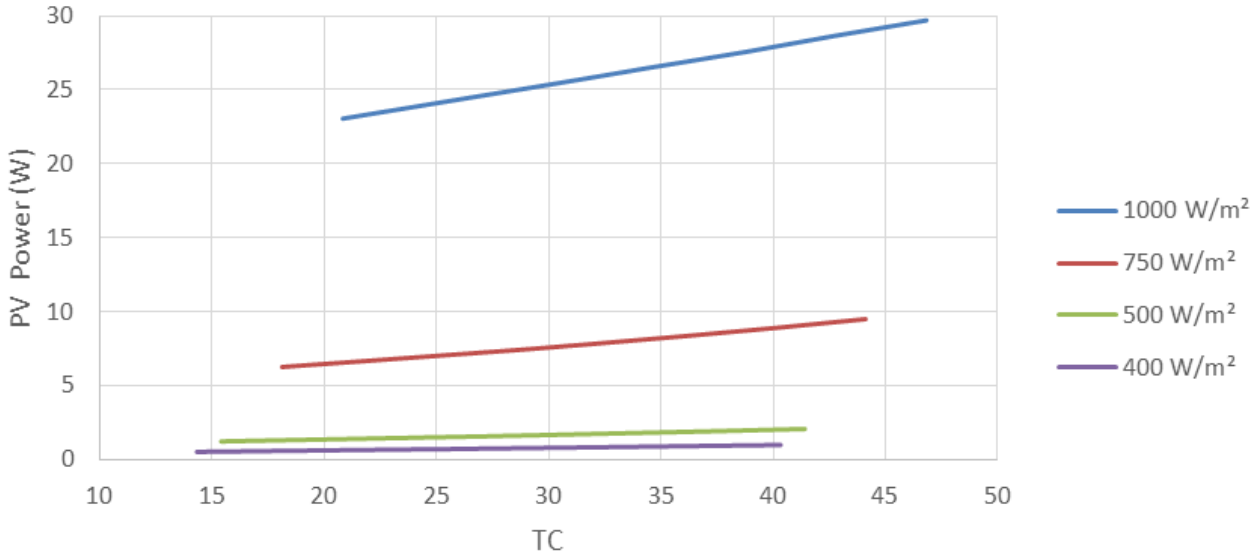

Figure-15. PV Characteristics: Power at different solar radiation

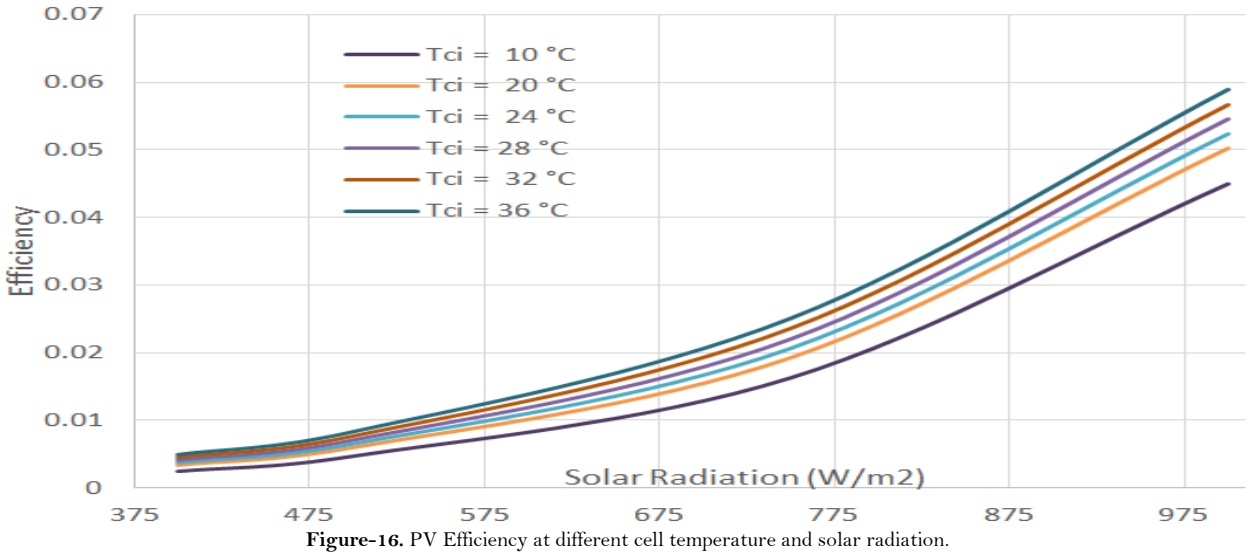

Figure-16. PV Efficiency at different cell temperature and solar radiation.

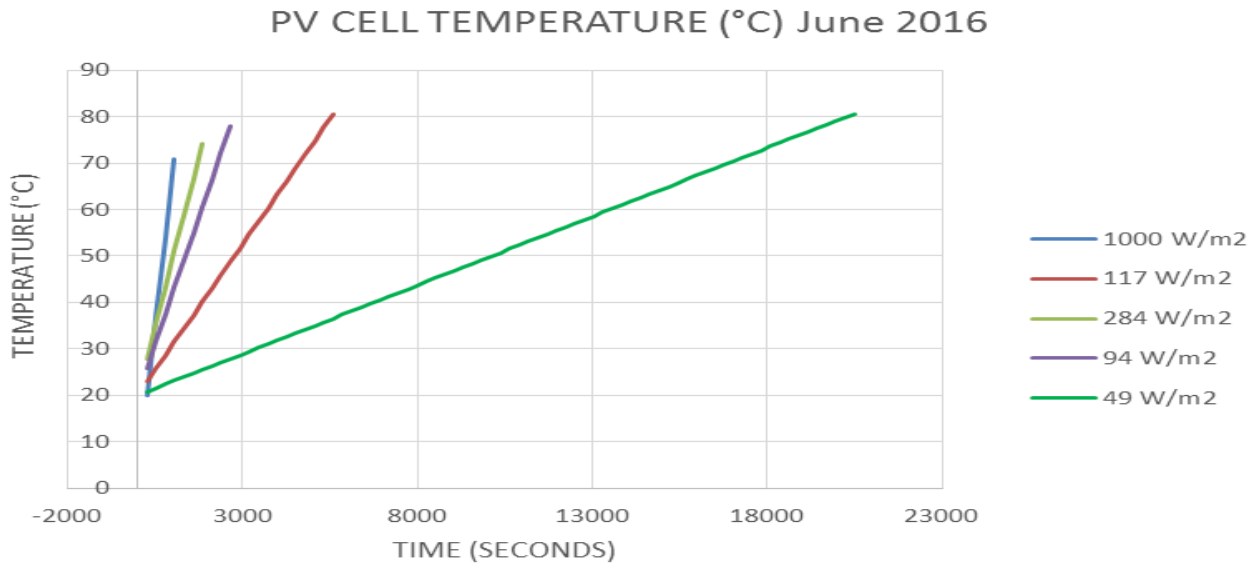

Figure-17. PV Characteristics: Time- variation of cell temperature

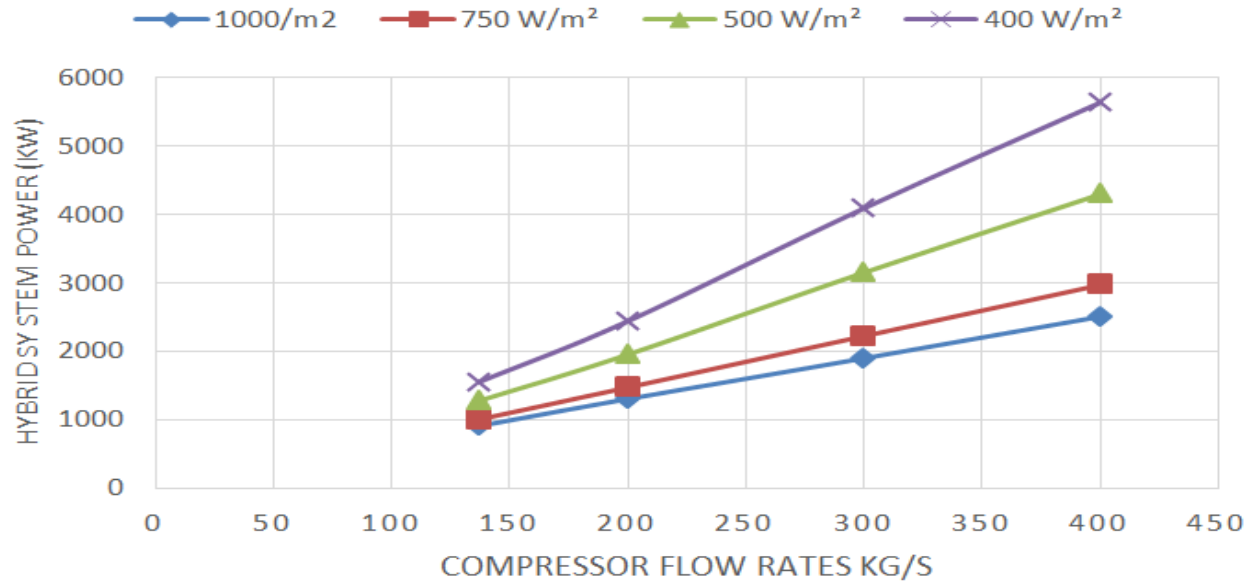

Figure-18. Hybrid system efficiency at different compressor air flow

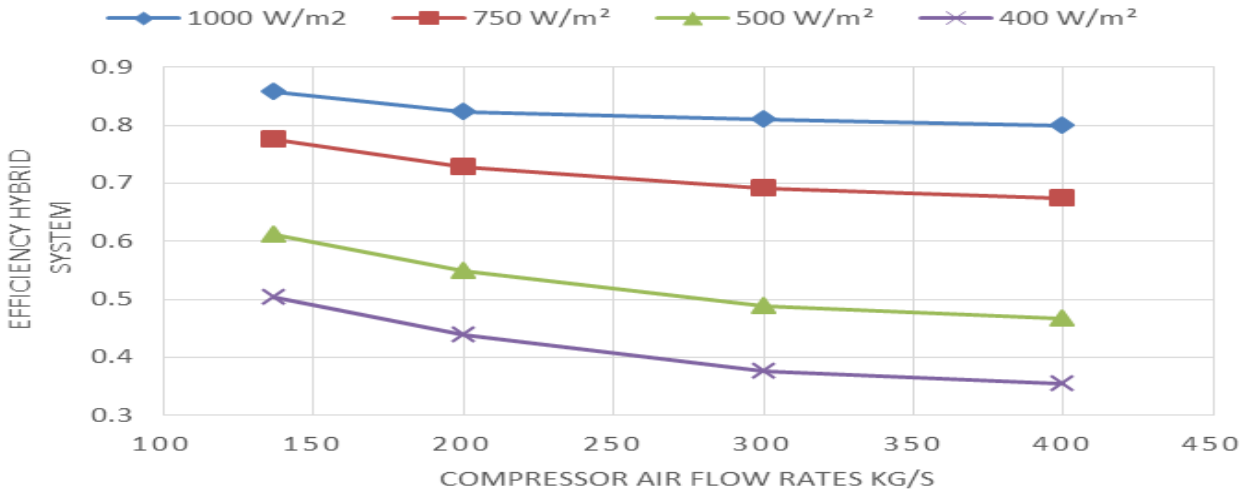

Figure-19. Hybrid system efficiency at different compressor air flow

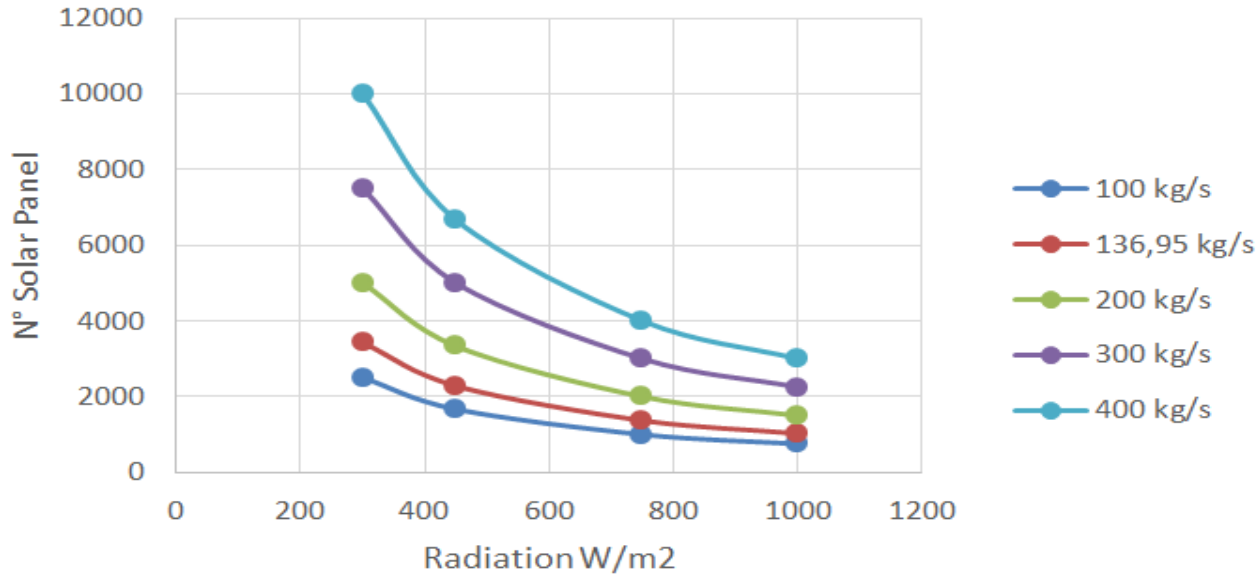

Figure-20. Number of solar panels at different compressor air flow rates

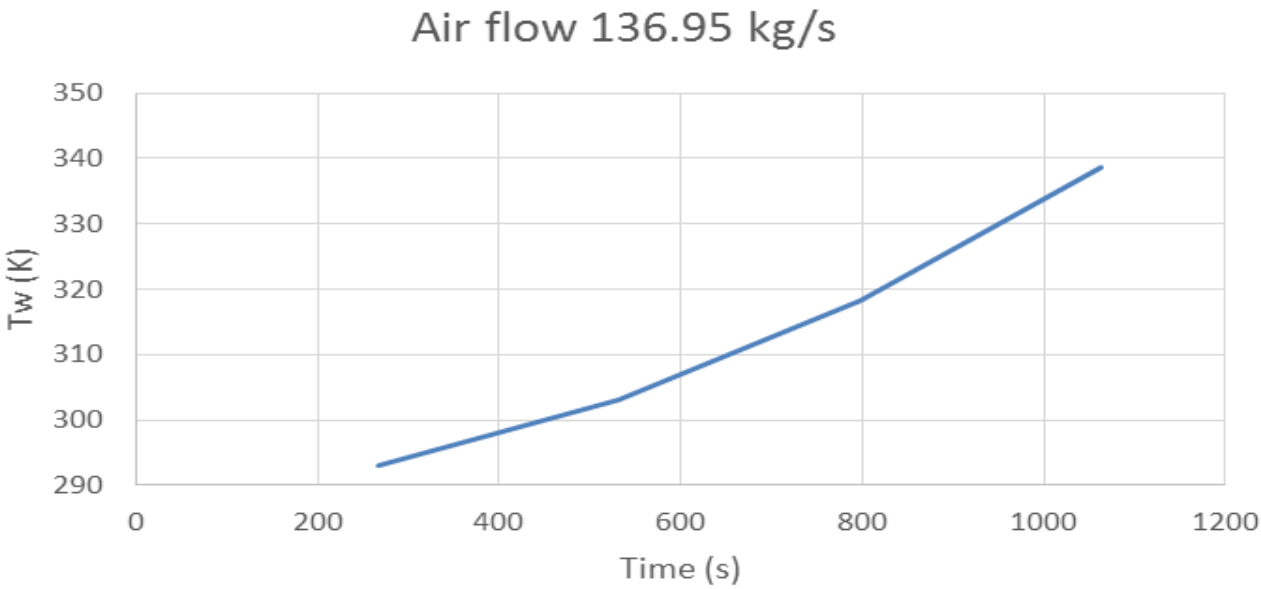

Figure-21. District heating Water temperature time-variation at 1000 w/m2 and 0% excess air

4.4. Numerical Model Validation

In order to validate our numerical model prediction described in equations (1 through 38), the system of equations were numerically coded and solved according to the Flow diagram displayed in Figure. 2. Data on PV cell temperature were unavailable in our laboratory. Therefore, the data presented by Fargali *et al.* (2008) were used for comparison purposes. The model predictions of the PV cell temperature were compared with data presented by Fargali *et al.* (2008) and presented in Figure 22. It has can be observed from this figure that some discrepancies exit. It is believed that the discrepancies are due to the fact that the Fargali *et al.* (2008) did not provide full disclosure of the various parameters and conditions of the PV cell temperature data. However, reference Rajapakse and Chungpaibulpantana (1994) had to be consulted on the various missing parameters in Fargali *et al.* (2008) in order to complete the validation presented in Figure. 22.

On the other hand, another attempt has been made to validate the PV solar panel output. Figure 23 displays the model's prediction of the electrical power at different amperages (Sami and Icaza, 2015) and compares against the

data of presented by reference (Ramon *et al.*, 2014) at solar radiation 750 w/m². It is quite evident from the data presented in this figure that the numerical model fairly predicted the data.

It is worthwhile noting that no data were available on the gas turbine for performance comparison; however, the predicted results of this particular model have been validated by reference (Fargali *et al.*, 2008; Chinda and Brault, 2012).

5. CONCLUSIONS

The energy conversion equations describing the heat and mass transfer mechanisms of a biogas gas turbine, solar PV and district heating hybrid system have been presented in time-variation formulations, integrated, coded and solved simultaneously. The results showed that increasing compressor air flow rate diminishes the hybrid system conversion efficiency. Furthermore, this study has shown that the biogas gas turbine output power is significantly influenced by the compressor entering temperature, air flow rates and obviously the excess air ratios.

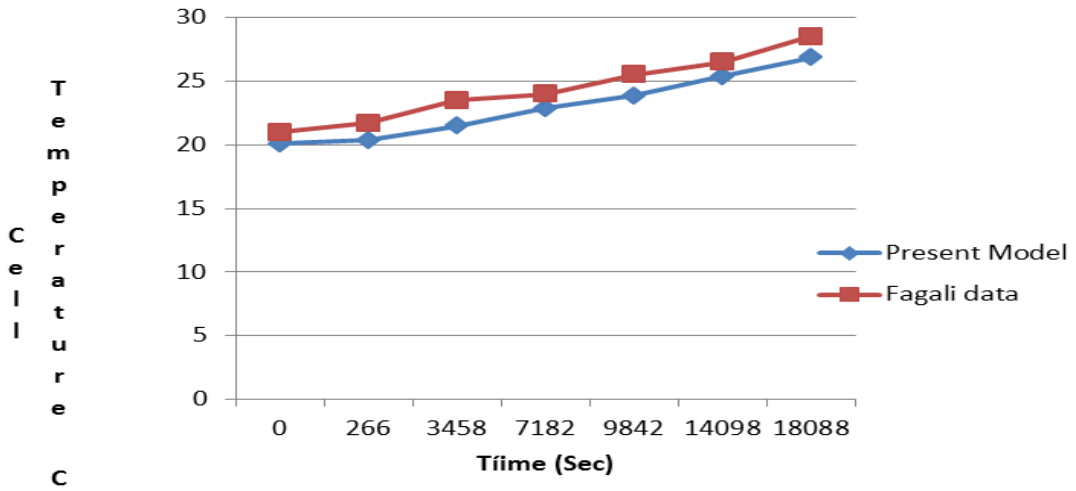

Figure-22. Comparison of predicted results by simulation model and data of Fargali *et al.* (2008)

On the other hand, the results presented hereby also demonstrated that the higher the compressor air flow rate the higher number of solar panel needed to drive the compressor. This is significant since the air flow rate impacts the output power at the gas turbine end and consequently the efficiency of the hybrid system.

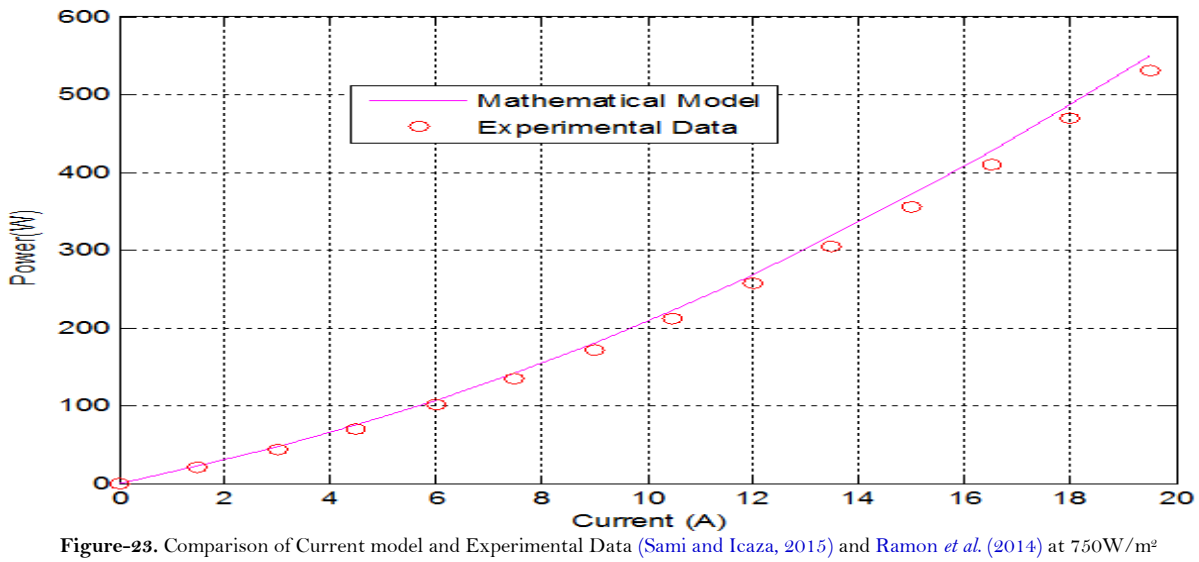

Figure-23. Comparison of Current model and Experimental Data (Sami and Icaza, 2015) and Ramon *et al.* (2014) at 750W/m²

On the other hand, the model in question also shows that the dynamic variation of the solar PV cell temperature should be observed to avoid disintegration and compromise of the solar PV heat transfer process. Finally, the proposed model predicted results compared fairly with data under various conditions and output power.

5.1. Nomenclature

A: Radiation surface area.
C_{p_w}: Specific heat of water
C_p: Specific heat of Flue gas
CV_{bio}: Calorific heat value of bio-gas
E_g: Stefan Boltzmann Coefficient
h_w: Convection heat transfer coefficient
m_{gas}: Mass flow rate of flue gas
m_{bio}: Biomass waste mass material
m_w: Mass flow rate water
Q_{comb}: Combustion heat added
Q_{rad}: Radiative heat
Q_{conv}: Convective heat
Q_{evap}: Evaporative heat
Q_{ed}: Building load
T: Temperature water in heat exchanger tank
t: Time variation.
V_{tank}: Volume of heater
W_{GTN}: Net Work generated at Gas turbine

5.2. Greek Alphabet

η_{bio}: Biomass combustion chamber efficiency
δ_w: Density of water
η_{TGU}: Efficiency of turbine generating unit

5.3. Subscripts

$comb$ –Combustion
$conv$ –Convection
$evap$ –Evaporation
gas –Flue gas
wl– water
rad –Radiation

Funding: The research work presented in this paper was made possible through the support of the Catholic University of Cuenca.
Competing Interests: The authors declare that they have no competing interests.
Contributors/Acknowledgement: All authors contributed equally to the conception and design of the study.

REFERENCES

Binayak, B., R.P. Shiva, L. Kyung-Tae and A. Sung-Hoon, 2014. Mathematical modeling of hybrid renewable energy system: A review on small hydro-solar-wind power generation. International Journal of Precision Engineering and Manufacturing-green Technology, 1(2): 157-173. *View at Google Scholar | View at Publisher*

Camerettia, M.C., G. Langellaa, S. Sabinoa and R. Tuccilloa, 2015. Modeling of a hybrid solar micro gas-turbine power plant. Energy Procedia, 82: 833 – 840. *View at Google Scholar | View at Publisher*

Chinda, P. and P. Brault, 2012. The hybrid solid oxide fuel cell (SOFC) and gas turbine (GT) systems steady state modeling. International Journal of Hydrogen Energy, 37(11): 9237-9248. *View at Google Scholar | View at Publisher*

Department of Energy, 2007. Potential benefits of distributed generation and rate related issues that may impede their expansion, a study pursuant to section 1817 of the energy policy act of 2005.

Fargali, H., F.H.M. Fahmy and M.A. Hassan, 2008. A simulation model for predicting the performance of PV/Wind- powered geothermal space heating system in Egypt. Online Journal on Electronics and Electrical Engineering, 2(4): 321-330. *View at Google Scholar*

Heller, P., M. Pfänder, T. Denk, F. Tellez, A. Valverde and J. Fernandez, 2006. Test and evaluation of a solar powered gas turbine system. Solar Energy, 80(10): 1225–1230. *View at Google Scholar | View at Publisher*

Jaber, J.O., 2004. Photovoltaic and gas turbine system for peak-demand applications. International Journal of Engineering and Technology, 1(1): 28-38. *View at Google Scholar*

Kavitha, S. and S.Y. Kamdi, 2013. Solar hydro hybrid energy system simulation. International Journal of Soft Computing and Engineering, 2(6): 500-503. *View at Google Scholar*

Korzynietz, R., M. Quero and R. Uhlig, 2012. SOLUGAS - future solar hybrid technology. Tech. Rep., Solar Paces. Retrieved from http://cms.solarpaces2012.org/proceedings/paper/7ee7e32ece8f2f8e0984d5ebff9d77b.

Mustafa, E., 2013. Sizing and simulation of PV-Wind hybrid power system. International Journal of Photoenergy, 2013: 1-10. *View at Google Scholar | View at Publisher*

Rajapakse, A. and S. Chungpaibulpantana, 1994. Dynamic simulation of a photovoltaic refrigeration system. RERIC International Energy Journal, 16(2): 67-101. *View at Google Scholar*

Ramon, A., A. Lopez, A. Maritz and G. Angarita, 2014. Parametros comparatives de celulas fotoelectricas para generaciob de energia: Implementacion de banco de pruebas usando DSP comparative parameters of solar cells for power generation: Test stand implementation using DSP. Ingeniería Energética, 35(3): 193- 201. *View at Google Scholar*

Sami, S. and D. Icaza, 2015. Modeling, simulation of hybrid solar photovoltaic, wind turbine and hydraulic power system. International Journal of Engineering Science and Technology, 7(9): 304-317. *View at Google Scholar*

Sami, S. and E. Marin, 2017. A numerical model for predicting performance of biomass and CHP hybrid system. IJESRT (In Press).

Saravanautto, H., G. Rogers and H. Chen, 2001. Gas turbine theory. 5th Edn., New York: Prentice Hall.

Sinai, J., C. Sugarmen and U. Fisher, 2005. Adaptation and modification of gas turbines for solar energy applications. In: Proceedings of GT2005 ASME Turbo Expo 2005.

Solgate, 2005. Solar hybrid gas turbine electric power system. Tech. Rep. EUR 21615, European Commission.

Yang, W., N. Hyung-sik and S. Choi, 2007. Improvement of operating conditions in waste incinerators using engineering tools. Waste Management, 27(5): 604-613. *View at Google Scholar | View at Publisher*

BIBLIOGRAPHY

www.bios-bioenergy.at.